PREPARATION AND OPERATIONS OF THE MISSION PERFORMANCE CENTRE (MPC) FOR THE COPERNICUS SENTINEL-3 MISSION

S3-A SLSTR Cyclic Performance Report

Cycle No. 021

Start date: 07/08/2017

End date: 03/09/2017

SENTINEL 3

Mission Performance Centre

Ref.: S3MPC.RAL.PR.02-021
Issue: 1.0
Date: 07/09/2017
Contract: 4000111836/14/I-LG

Customer:	ESA	**Document Ref.:**	S3MPC.RAL.PR.02-021
Contract No.:	4000111836/14/I-LG	**Date:**	07/09/2017
		Issue:	1.0

Project:	PREPARATION AND OPERATIONS OF THE MISSION PERFORMANCE CENTRE (MPC) FOR THE COPERNICUS SENTINEL-3 MISSION		
Title:	S3-A SLSTR Cyclic Performance Report		
Author(s):	SLSTR ESLs		
Approved by:	D. Smith, SLSTR ESL Coordinator	**Authorized by**	Frédéric Rouffi, OPT Technical Performance Manager
Distribution:	ESA, EUMETSAT, S3MPC consortium		
Accepted by ESA	S. Dransfeld, MPC Deputy TO for OPT P. Féménias, MPC TO		
Filename	S3MPC.RAL.PR.02-021 - i1r0 - SLSTR Cyclic Report 021.docx		

Changes Log

Version	Date	Changes
1.0	07/09/2017	First Version

List of Changes

Version	Section	Answers to RID	Changes

Table of content

List of Figures

1 Instrument monitoring

1.1 Instrument temperatures

- Instrument temperatures were stable and consistent with expected values following the decontamination phase which was performed towards the end of Cycle 20.
- Blackbody, baffle and OME temperatures peaked at the beginning of the year when the Earth was at perihelion. In cycle 21, the blackbody temperatures were stable at their expected values.

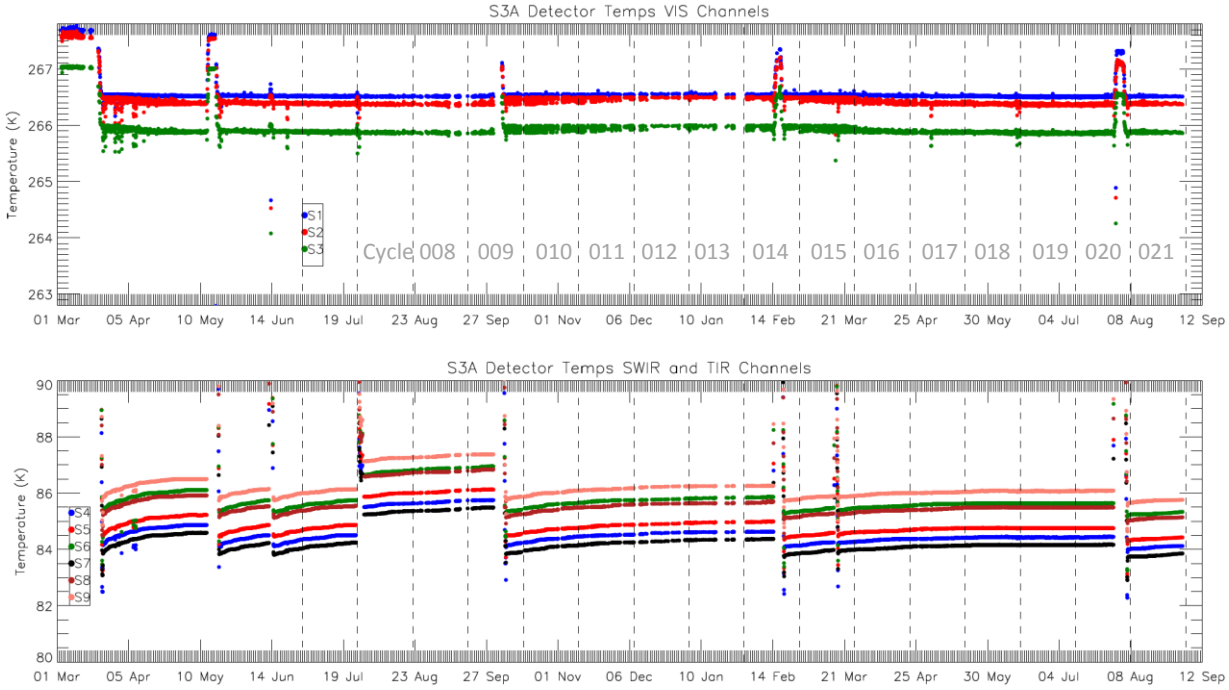

Figure 1: Detector temperatures for each channel from 1st March 2016. Discontinuities occur for the infrared channels where the FPA was heated for decontamination or following an anomaly. The vertical dashed lines indicate the start and end of each cycle.

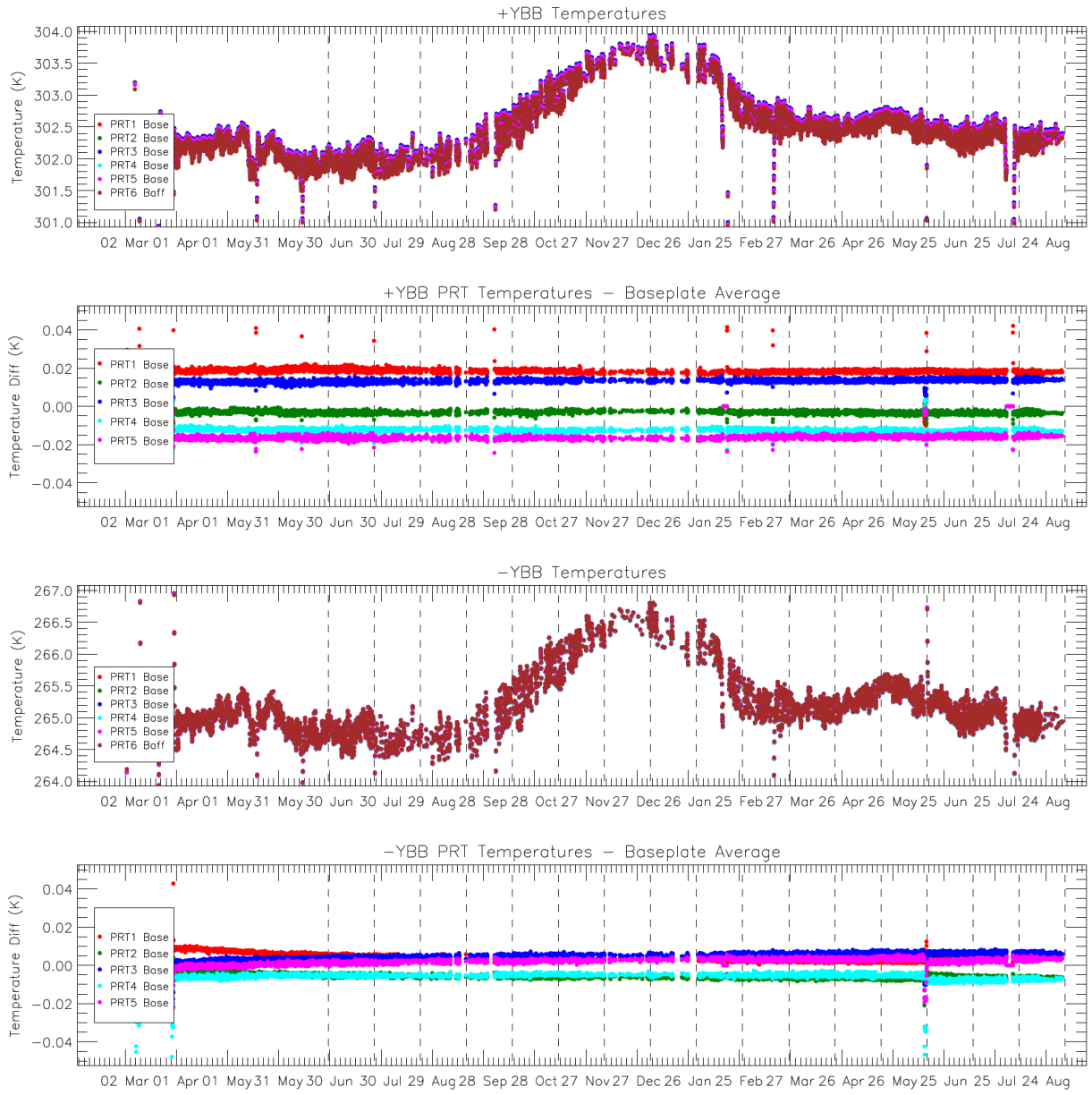

Figure 2: Blackbody temperature and baseplate gradient trends. The vertical dashed lines indicate the start and end of each cycle.

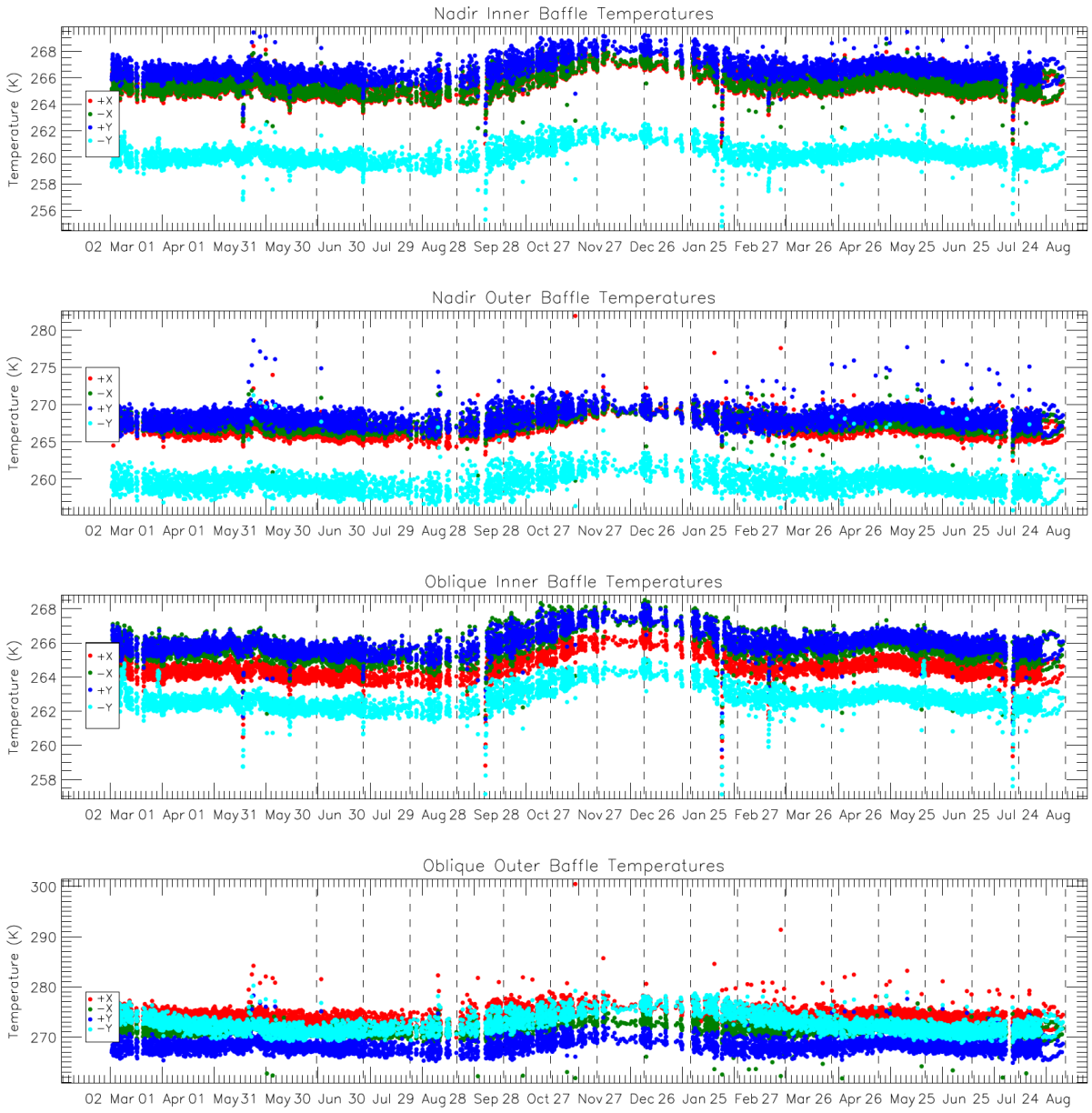

Figure 3: Baffle temperature trends. The vertical dashed lines indicate the start and end of each cycle.

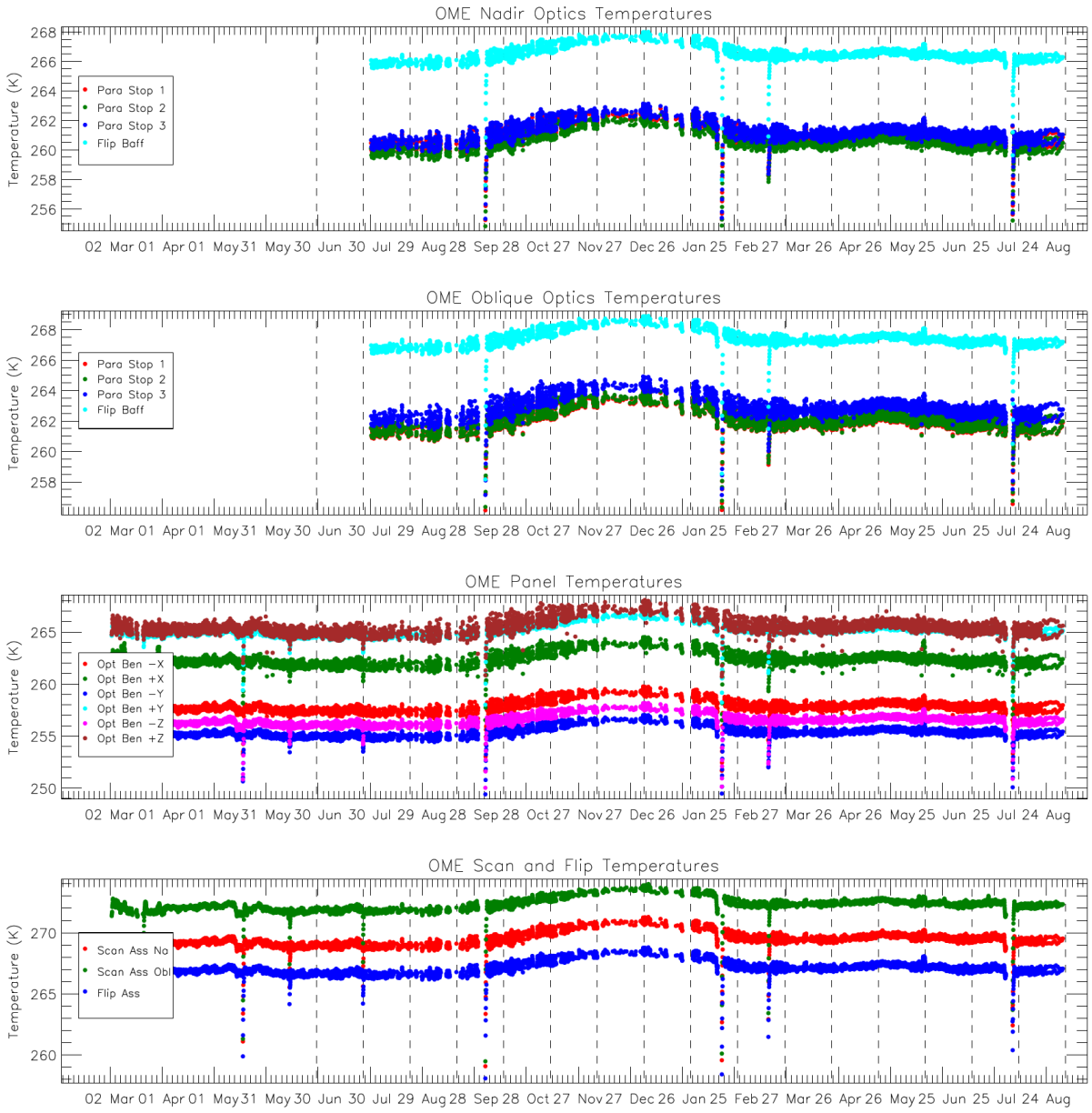

Figure 4: OME temperature trends showing the paraboloid stops and flip baffle (top two plots) and optical bench and scanner and flip assembly (lower two plots). The top two plots only show data starting from 30th July 2016. The vertical dashed lines indicate the start and end of each cycle.

1.2 Scanner performance

Scanner performance has been consistent with previous operations and within required limits.

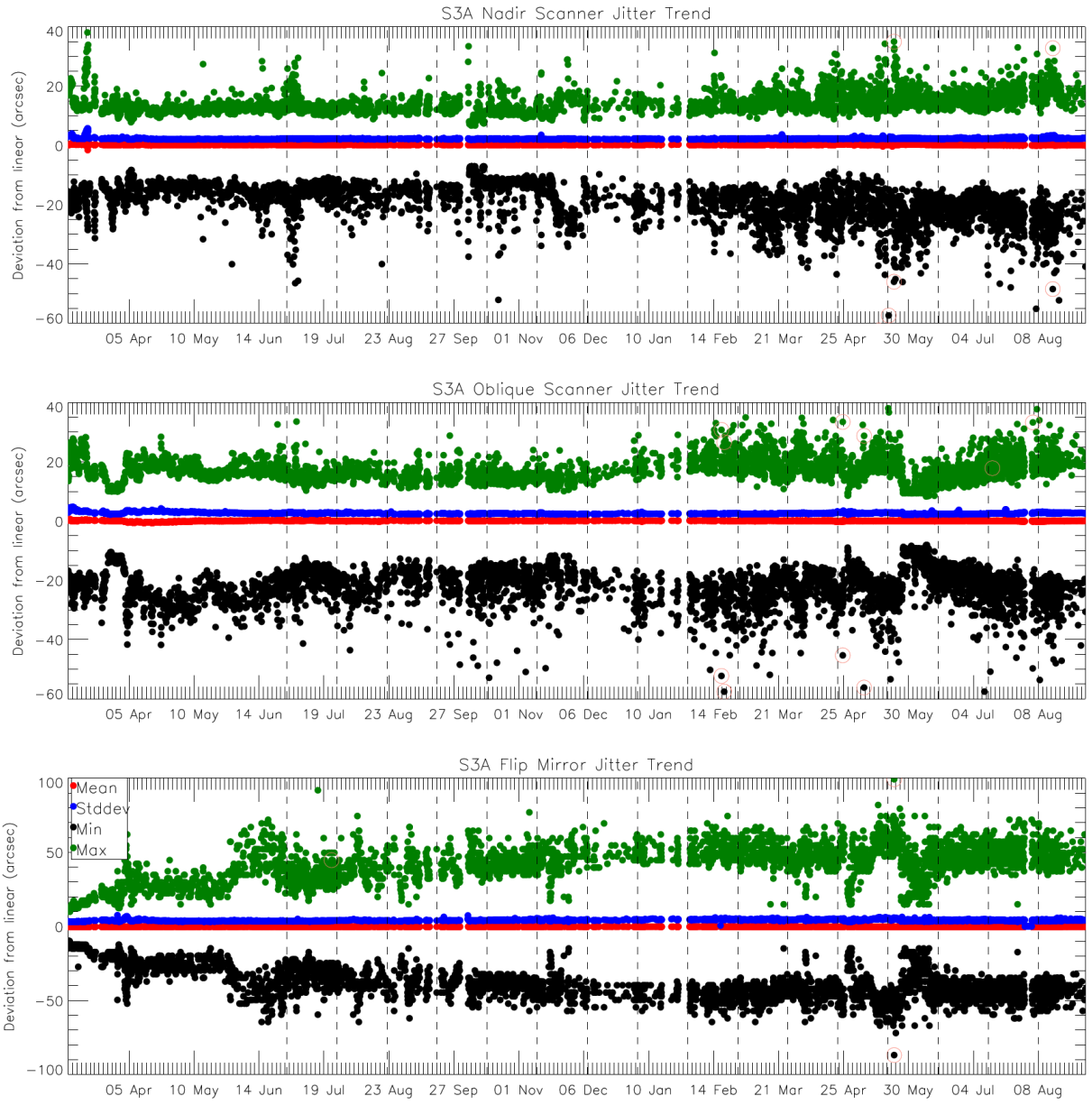

Figure 5: Scanner and flip jitter, showing mean, stddev and max/min position compared to the expected one for the nadir view. The vertical dashed lines indicate the start and end of each cycle.

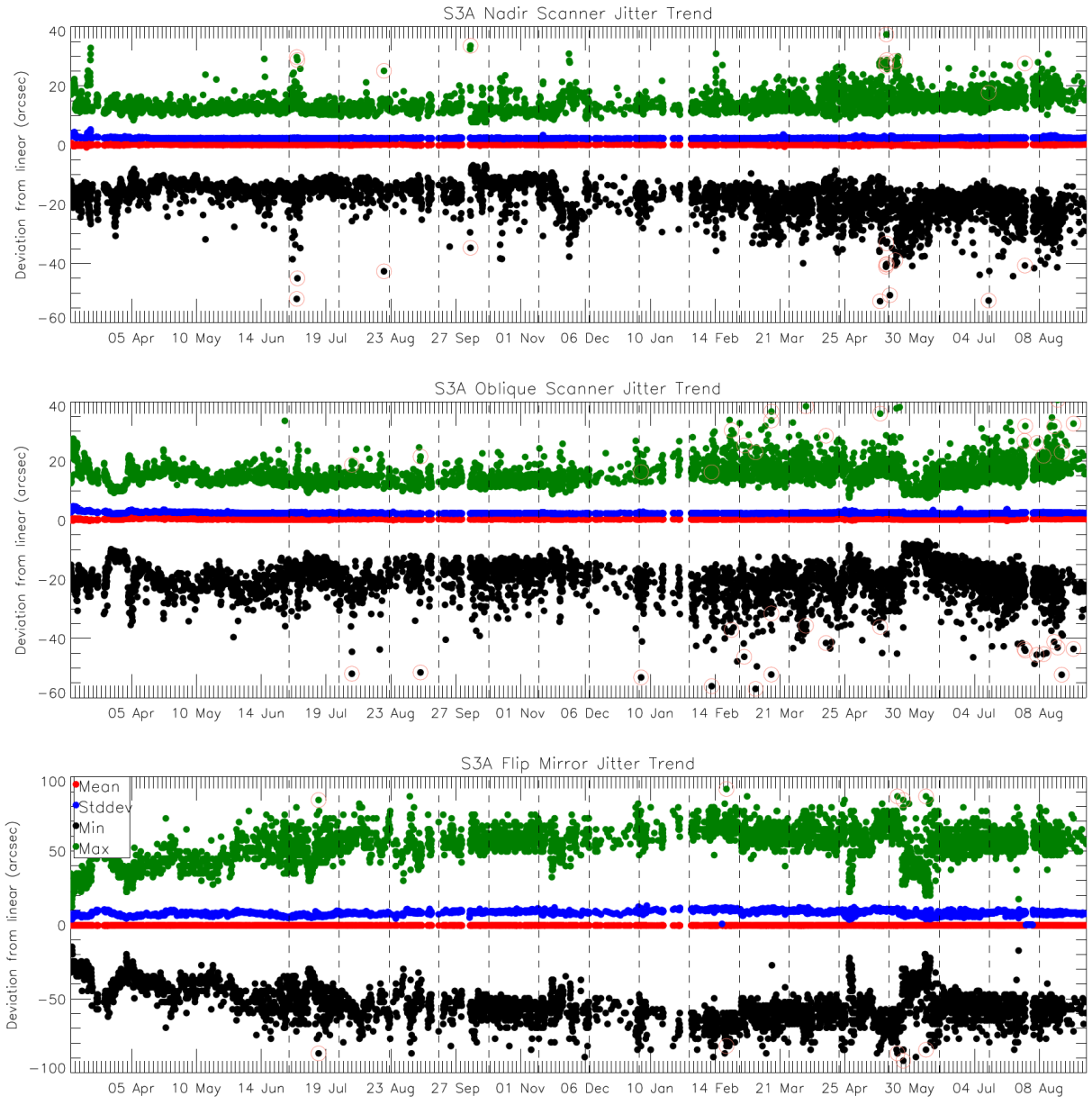

Figure 6: Scanner and flip jitter, showing mean, stddev and max/min position compared to the expected one for the oblique view. The vertical dashed lines indicate the start and end of each cycle.

1.3 Detector noise levels

1.3.1 VIS and SWIR channel signal-to-noise

The VIS and SWIR channel noise was stable and consistent with previous operations - the signal-to-noise ratio of the measured VISCAL signal is plotted in Figure 7. Table 1 and Table 2 give the average signal-to-noise in each cycle (excluding the anomaly/decontamination period in Cycle 20). Note that this averages over the significant detector-detector dispersion for the SWIR channels that is shown in Figure 7.

Table 1: Average reflectance factor, and signal-to-noise ratio of the measured VISCAL signal for cycles 010-021, averaged over all detectors for the nadir view.

	Average Reflectance Factor	Nadir Signal-to-noise ratio											
		Cycle 010	Cycle 011	Cycle 012	Cycle 013	Cycle 014	Cycle 015	Cycle 016	Cycle 017	Cycle 018	Cycle 019	Cycle 020	Cycle 021
S1	0.187	236	235	233	226	217	224	233	234	231	229	233	231
S2	0.194	238	238	236	234	227	230	236	236	232	231	235	235
S3	0.190	238	239	235	230	221	230	236	238	228	231	230	229
S4	0.191	141	145	141	139	137	139	142	140	140	139	137	135
S5	0.193	236	235	238	234	234	233	233	235	236	233	232	232
S6	0.175	143	147	145	143	141	144	142	143	143	142	140	136

Table 2: Average reflectance factor, and signal-to-noise ratio of the measured VISCAL signal for cycles 010-021, averaged over all detectors for the oblique view.

	Average Reflectance Factor	Oblique Signal-to-noise ratio											
		Cycle 010	Cycle 011	Cycle 012	Cycle 013	Cycle 014	Cycle 015	Cycle 016	Cycle 017	Cycle 018	Cycle 019	Cycle 020	Cycle 021
S1	0.166	249	249	247	238	229	236	243	247	246	242	241	241
S2	0.170	254	253	250	241	232	241	248	251	249	247	247	244
S3	0.168	251	251	244	237	227	236	245	249	244	242	239	234
S4	0.166	109	112	112	108	107	108	108	111	110	109	108	108
S5	0.166	173	173	173	169	169	172	169	169	171	168	168	168
S6	0.155	110	114	113	105	106	107	109	109	110	108	106	108

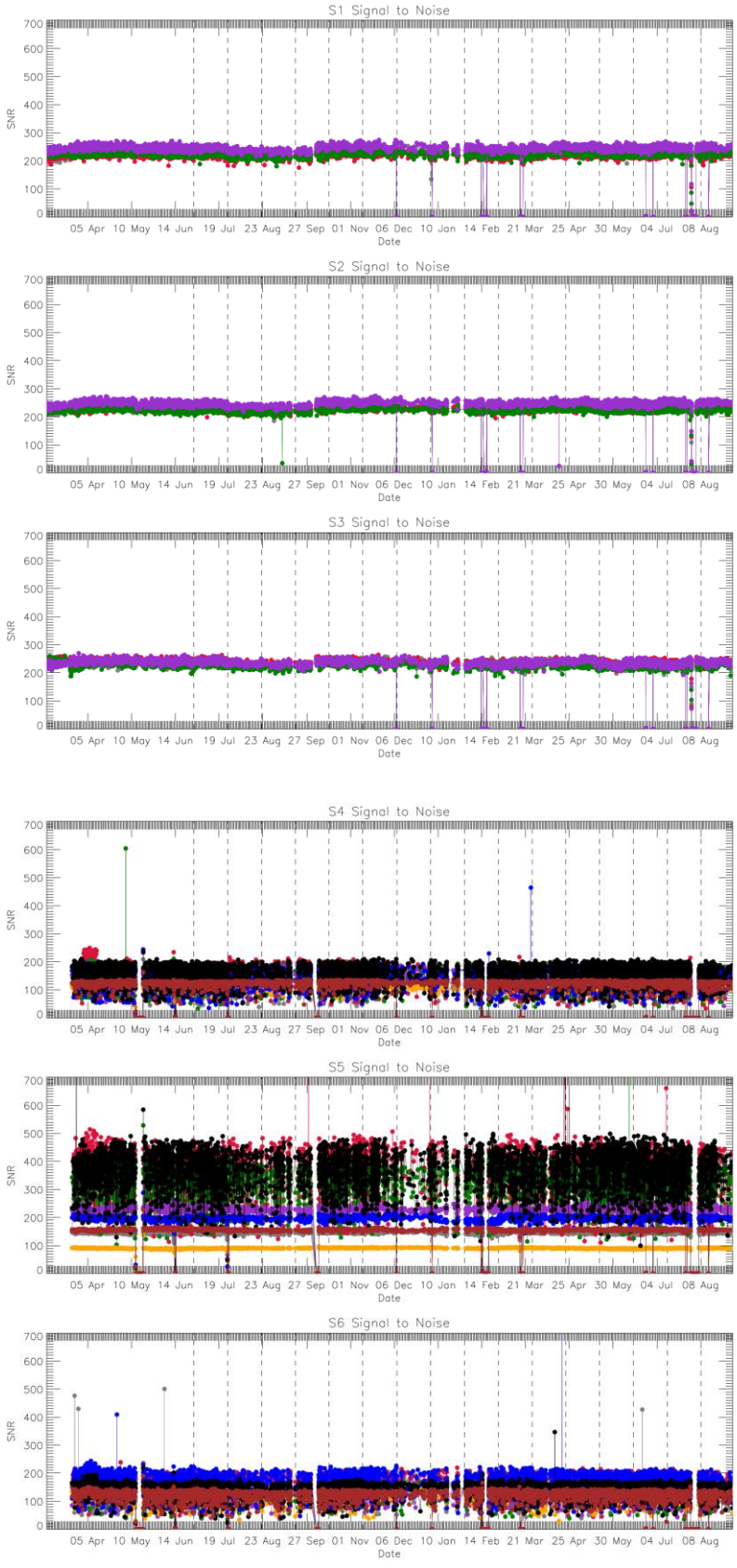

Figure 7: VIS and SWIR channel signal-to-noise of the measured VISCAL signal in each orbit. Different colours indicate different detectors.

1.3.2 TIR channel NEDT

The thermal channel NEDT values are consistent with previous operations and within the requirements. NEDT values for each cycle, averaged over all detectors and both Earth views, are shown in Table 3 and Table 4.

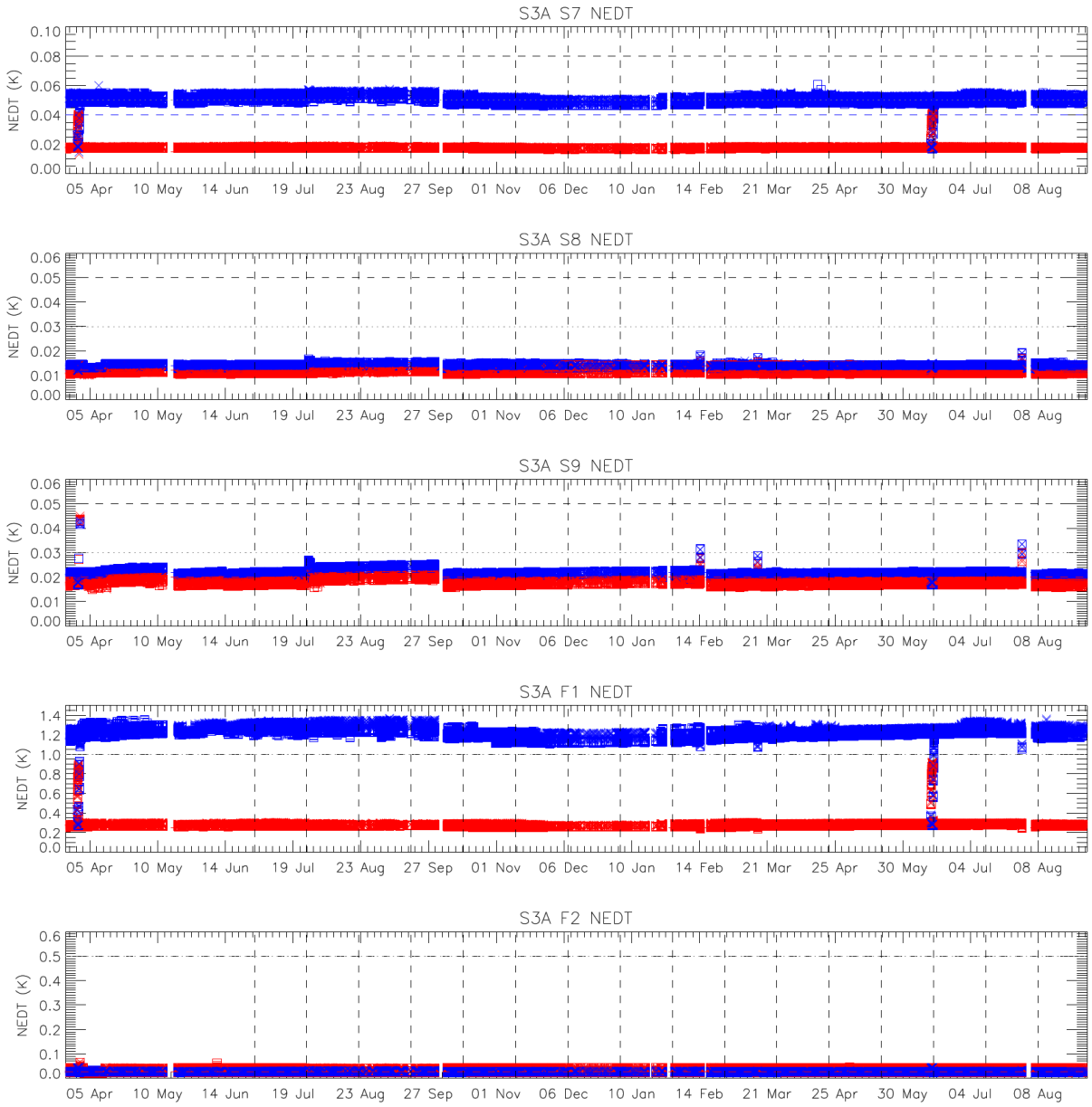

Figure 8: NEDT trend for the thermal channels. Blue points were calculated from the cold blackbody signal and red points from the hot blackbody. Horizontal lines indicate the requirement (dashed) and goal (dotted) as well as the measured values on ground (red and blue dashed).

Table 3: NEDT for cycles 010-021 averaged over all detectors for both Earth views towards the +YBB (hot).

		Cycle 010	Cycle 011	Cycle 012	Cycle 013	Cycle 014	Cycle 015	Cycle 016	Cycle 017	Cycle 018	Cycle 019	Cycle 020	Cycle 021
+YBB temp (K)		302.822	303.289	303.680	303.621	303.206	302.674	302.544	302.541	302.593	302.386	302.348	302.307
NEDT (mK)	**S7**	17.2	16.9	16.9	16.8	16.9	17.2	17.2	17.2	18.1	17.2	17.2	17.1
	S8	10.9	11.0	11.0	11.1	11.0	10.9	10.9	11.0	11.1	11.0	11.1	10.9
	S9	17.1	17.4	17.7	17.9	17.6	17.0	17.0	17.2	17.5	17.4	17.5	16.7
	F1	265	260	260	260	260	268	268	271	297	276	276	269
	F2	27.5	27.7	28.0	28.0	27.9	27.6	27.6	27.8	27.8	27.8	27.8	27.3

Table 4: NEDT for cycles 010-021 averaged over all detectors for both Earth views towards the –YBB (cold).

		Cycle 010	Cycle 011	Cycle 012	Cycle 013	Cycle 014	Cycle 015	Cycle 016	Cycle 017	Cycle 018	Cycle 019	Cycle 020	Cycle 021
-YBB temp (K)		265.575	266.112	266.512	266.353	265.807	265.183	265.136	265.260	265.412	265.125	265.000	264.902
NEDT (mK)	**S7**	48.1	47.2	46.6	46.8	47.9	48.7	49.0	48.8	46.9	49.1	49.5	49.5
	S8	14.4	14.4	14.5	14.4	14.4	14.2	14.2	14.3	14.2	14.3	14.4	14.2
	S9	21.5	21.8	22.2	22.4	22.1	21.3	21.4	21.6	21.6	21.9	22.0	21.1
	F1	1209	1162	1123	1130	1178	1222	1191	1199	1163	1229	1235	1212
	F2	29.3	29.5	29.6	29.6	29.6	29.2	29.3	29.3	29.4	29.6	29.7	29.2

1.4 Calibration factors

1.4.1 VIS and SWIR VISCAL signal response

Signals from the VISCAL source for the VIS channels show oscillations due to the build up of ice on the optical path within the FPA. Decontamination must be carried out periodically in order to warm up the FPA and remove the ice. The latest decontamination cycle was successfully performed in Cycle 20 following the anomaly on 30th July. The VISCAL signal has returned to its expected value following the decontamination.

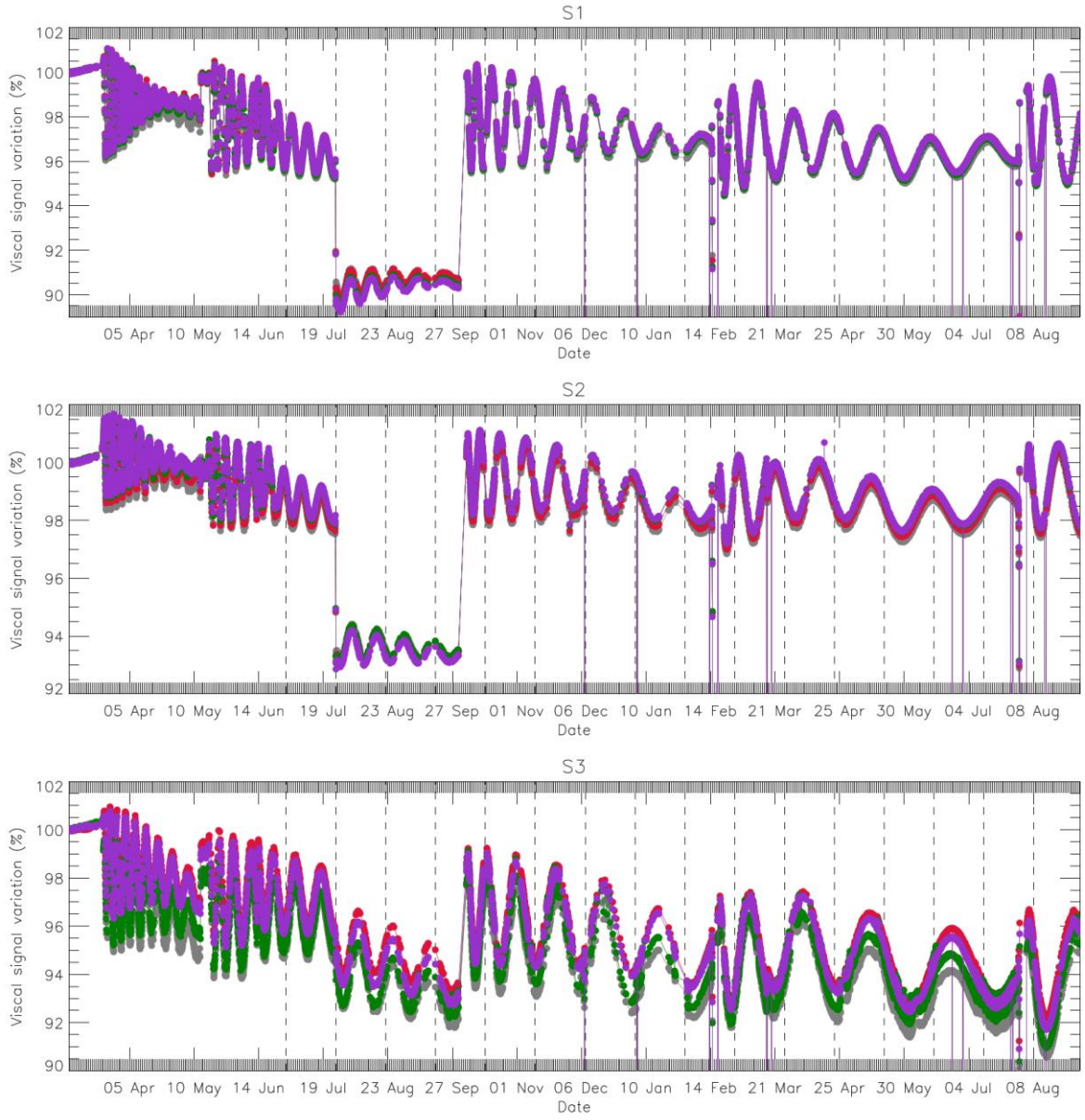

Figure 9: VISCAL signal trend for VIS channels (nadir view).

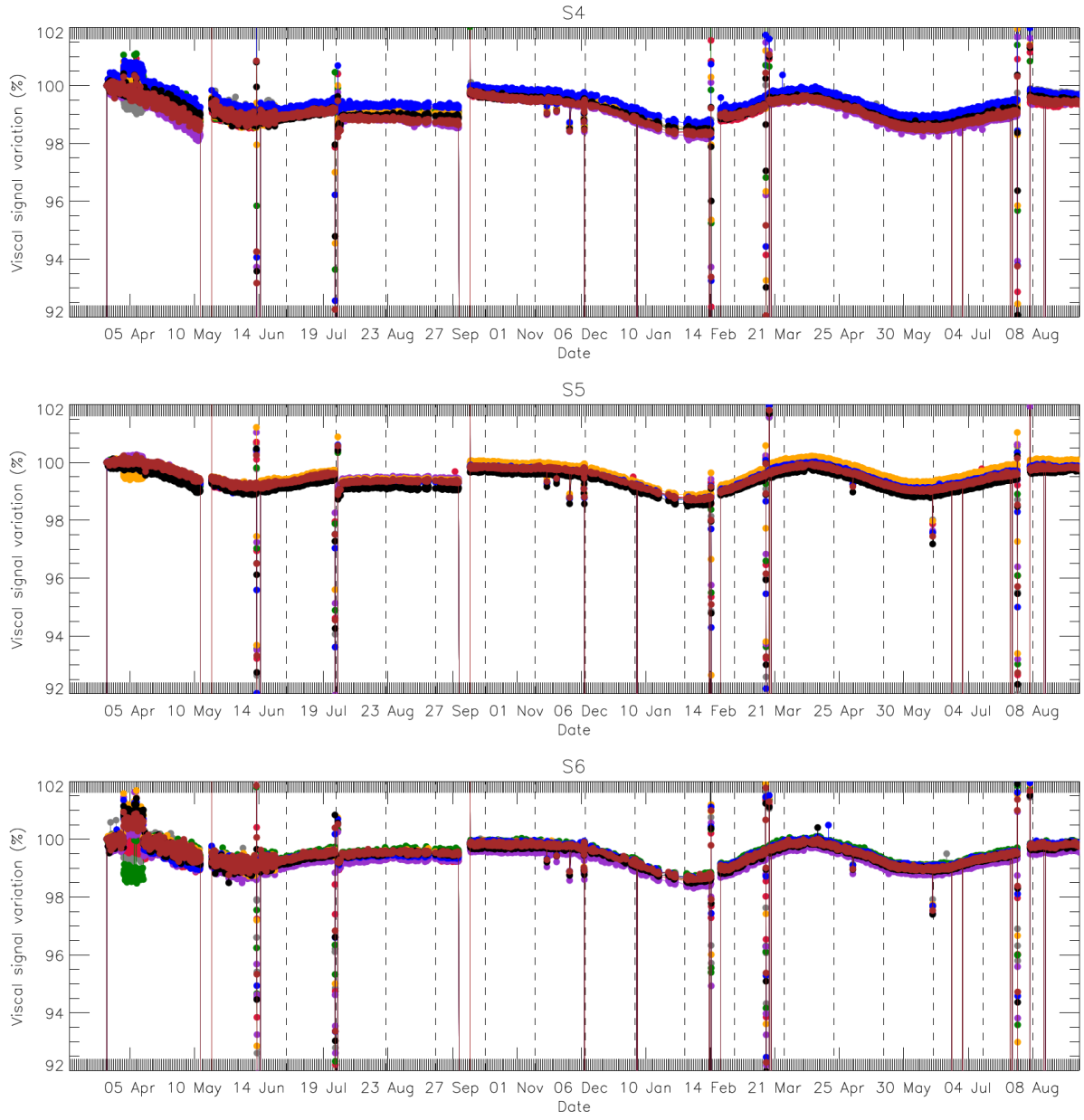

Figure 10: VISCAL signal trend for SWIR channels (nadir view).

2 Events

SLSTR was switched on and operating nominally during the cycle, with SUE scanning and autonomous switching between day and night modes.

3 Appendix A

Other reports related to the Optical mission are:

- S3-A OLCI Cyclic Performance Report, Cycle No. 021 (ref. S3MPC.ACR.PR.01-021)

All Cyclic Performance Reports are available on MPC pages in Sentinel Online website, at: https://sentinel.esa.int

End of document